Tunnelling and Underground Space Technology 126 (2022) 104552

Contents lists available at ScienceDirect

Tunnelling and Underground Space Technology incorporating Trenchless Technology Research

journal homepage: www.elsevier.com/locate/tust

Trenchless technology research

Thermo-hydro-mechanical response of a partially sealed circular tunnel in saturated rock under inner water pressure

Minjie Wen [a,*], Houren Xiong [b], Jinming Xu [c]

[a] Research Center of Coastal Urban Geotechnical Engineering, Zhejiang University, Hangzhou, Zhejiang 310058, PR China
[b] College of Engineering and Architecture, Jiaxing University, Jiaxing 314001, PR China
[c] Department of Civil Engineering, Shanghai University, Shanghai, 200072, PR China

ARTICLE INFO

Keywords:
Saturated rock
Flexible porous materials
Coupled thermo-hydro-mechanical response
Partially permeable
Stress coefficient
Laplace transform

ABSTRACT

The thermo-hydro-mechanical response of a partially sealed circular tunnel in saturated rock subject to inner water pressure with high temperature is investigated by the fully coupling thermo-hydro-mechanical model. The tunnel is assumed to be partially sealed, and the partially permeable condition of the boundary of tunnel is established using the Darcy' law. Furthermore, a stress coefficient depending on the volume fraction of the pore fluid is quoted to establish the stress coordination conditions at the boundary of tunnel, and the solutions of temperature increment, displacement, pore water pressure and stress are obtained in the domain of Laplace transform. Based on the Crump method taking inverse Laplace transform, the numerical solution to the problem is presented. Numerical results are displayed graphically and analyzed in detail.

1. Introduction

Dynamic behaviors of pressure tunnels have always been a hot issue that attracts a great deal of attention from scholars in the field of geotechnical engineering. Many researchers have obtained tunnels' dynamic response to internal loads under permeable or impermeable boundary conditions (Gao et al., 2013; Gao et al., 2016; Lu et al., 2007; Senjuntichai and Rajapakse, 2010; Xia et al., 2017). In practical engineering applications, concrete tunnel lining materials are typical kinds of porous materials with finite permeability, forming seepage field in the stratum. Therefore, Li believed that tunnel boundaries have partially permeable states; according to Darcy's Law, some permeable boundary conditions were constructed (Li, 1999). On that basis, Liu *et al.* analyzed the relative permeability of the surrounding rocks and linings and the endurance of inner water pressure (Liu et al., 2010c). Nevertheless, when the surrounding rocks and linings are subjected to inner water pressure with high temperature, the pore fluid, stress and temperature can interact in the rock. That is, there are coupling effects between heat (temperature field), flow (seepage field), and forces (stress field and displacement field). These can deform the surrounding rock and lining, and even cause failure. Therefore, investigating the coupled thermo-hydro-mechanical dynamic response of tunnels' linings in saturated rock under inner water pressure action is of great significance. It can provide certain theoretical foundations and engineering guidance for design of tunnels for stability, and calculation of pressure tunnels' performance characteristic.

Biot proposed the coupled thermoelastic theory to eliminate the paradox that the elastic change has no effect on the temperature in the classical uncoupled theory. However, Biot's thermoelastic coupling model based on Fourier heat conduction law can only predict infinite heat propagation velocity (Biot, 1977). Therefore, many scholars modified the traditional Fourier's law of heat conduction, to establish a model for predicting the propagation of a thermal wave with a finite velocity. Lord and Shulman formulated a generalized theory of thermoelasticity by incorporating a flux-rate term into Fourier's law of heat conduction (Lord and Shulman, 1967). Green and Lindsay developed a temperature-rate-dependent thermoelasticity that includes two thermal relaxation times (Green and Lindsay, 1972). Green and Naghdi introduced the theory of thermoelasticity without energy dissipation (Green and Naghdi, 1993). There are other generalized thermoelasticity theories such as two-temperature generalized thermoelasticity (Youssef, 2011) and fractional order theory of thermoelasticity (Ezzat, 2011). All these theories have been used extensively for analyzing semi-infinite half space, spherical cavities, and cylinders (Abouelregal, 2013; Hamza et al., 2014; Hamza et al., 2016; Kundu and Mukhopadhyay, 2005; Xia et al., 2009). It should be noted that the effects of pores and

* Corresponding author.
E-mail address: 7279026@163.com (M. Wen).

https://doi.org/10.1016/j.tust.2022.104552
Received 13 March 2019; Received in revised form 22 May 2021; Accepted 12 April 2022

pore water were mostly neglected in the above studies.

However, rocks are always porous medium in practical engineering applications, which can lead to coupling effects between temperature, force and seepage under inner water pressure. Studies based on saturated porous medium models are more aligned with practical conditions. Bai *et al.* established the mathematical model for full thermo-hydro-mechanical coupling, and analyzed the thermal consolidation problem of saturated porous medium with spherical cavities (Bai and Li, 2013). Based on the Biot's consolidation theory, Darcy's law, and the modified Fourier heat conduction equation, Liu *et al.* constructed a full coupling thermo-hydro-mechanical dynamic model (Liu et al., 2009) and then used it to examine the dynamic response of saturated porous thermoelastic media with spherical cavities and cylindrical pores (Liu et al., 2010a; Liu et al., 2010b). Moreover, the results of the above analysis were compared with the results from a hydro-mechanical coupling dynamic model. Taking relaxation effects into account, Sherief and Hussein established a thermo-fluid-solid dynamic model of saturated porous media with two temperatures and analyzed transient responses of semi-infinite bodies (Sherief and Hussein, 2012). On that basis, Ezzat *et al.* constructed a coupling thermo-hydro-mechanical dynamic model of saturated porous materials with a fractional derivative with respect to time, and examined dynamic response of semi-infinite porous medium under thermal shock (Ezzat and Ezzat, 2016). Based on porous media theory, Yang *et al.* established a coupling thermo-hydro-mechanical dynamic model under local thermal non-equilibrium conditions and the related variational principle (Yang, 2005). By introducing the concept of a mean weighted temperature, He et al. derived a coupling thermo-hydro-mechanical model under local thermal non-equilibrium conditions and analyzed the transient response of saturated porous medi with spherical cavity (He and Yang, 2009). Abousleiman and Ekbote focused on the transient dynamic response of saturated transverse isotropic soil (Abousleiman and Ekbote, 2005). After considering thermo-hydro-mechanical coupling effects, Xiong *et al.* employed the regular modal method for investigating the dynamic response of saturated porous foundation soil and analyzed the effect of loading frequency changes on various physical characteristics of the foundation (Xiong et al., 2018). Although the studies based on porous thermoelastic theory achieved greater progress than those based on thermoelastic theory, most of these analyses were performed based on uncoupling or partial coupling theory in view of the complexity of the governing equations. These scholars still addressed coupling thermo-hydro-mechanical issues using Fourier heat conduction law. That is, thermo-hydro-mechanical analysis in real sense has yet to be realized (Bai and Abousleiman, 1997; Blond et al., 2003).

Li *et al.* employed Darcy's law to establish partly permeable boundary conditions for calculations of tunnel pressure (Li, 1999). Xie and Liu also led their teams to examine the dynamic responses of partially permeable tunnel and spherical cavity in saturated porous media under axisymmetric load and fluid pressure (Liu and Xie, 2005; Xie et al., 2004). In this study, considering the full effects of thermo-hydro-mechanical coupling, the lining and rock can be regarded as flexible porous elastic materials and saturated porous thermoelastic medium. Based on generalized thermoelastic theory, a mathematic model for the full coupled thermo-hydro-mechanical was established, and the dynamic responses of partially permeable cylindrical lined tunnel in saturated rock when the tunnel boundary was under inner water pressure with high temperature were investigated. Then, the expressions of temperature increments, pore water pressure and displacement were derived using the Laplace transform and the Cayley-Hamilton law. The tunnel was assumed to be partially sealed; the partially permeable conditions of the boundary of tunnel were established using the Darcy' law. Furthermore, a stress coefficient depending on the volume fraction of the pore fluid was quoted to establish the stress coordination conditions at the boundary of tunnel, and the solutions of temperature increment, displacement, pore water pressure and stress were obtained in the domain of Laplace transform. Finally, the corresponding numerical solutions were obtained using the Crump inversion method of taking the inverse Laplace transform, and the effects of the stress and permeability coefficients on the thermo-hydro-mechanical response of a partially sealed circular tunnel were studied.

2. Mathematical model

As shown in Fig. 1, there exists a cylindrical lining tunnel, with an inner radius of R_1 and an external radius of R_2, in infinite rock. A time-dependent inner water pressure with high temperature acts on the tunnel boundary, which can be equivalent to a combination of a heat source and mechanical source. In practical engineering, tunnels are generally supported by their lining structure and the lining is generally made up of concrete. The surrounding infinite rock and lining can be treated as a saturated porous thermoelastic media. Li *et al.* pointed out that the tunnel is in semi-closed state (Li, 1999), i.e., the boundary is partly permeable. In practical engineering, the lining thickness h is far smaller than the tunnel radius, and the lining can be regarded as a kind of fully flexible material. That is, the elastic modulus approaches 0 ($E_l \to 0$). By assuming that the tunnel is infinitely long, the system can be treated as plane strain model in further analysis. The lining and rock are in close contact with each other; they exhibit small deformations and no relative slippage.

3. Thermo-hydro-elastodynamic response of saturated rock

Assuming the rock to be a linear-elastic, isotropic, saturated porous medium and by considering the effect of deformation on the balance of mass and heat, the dynamic equation of the saturated rock can be expressed as (Liu et al., 2010a):

$$(\lambda+2\mu)\nabla^2 e-\alpha\nabla^2 p-\lambda'\nabla^2\left(\theta+\tau_1\frac{\partial\theta}{\partial t}\right)=(\rho-\rho_w\alpha)\frac{\partial^2 e}{\partial t^2}+\rho_w a_c\frac{\partial^2\theta}{\partial t^2}-\frac{\rho_w}{M}\frac{\partial^2 p}{\partial t^2} \tag{1}$$

where, $e=\partial(ru_r)/r\partial r$ is the bulk strain of the porous medium.u_r,p are the radial displacement and pore water pressure, respectively. θ is temperature increment ($\theta = T-T_0$, T is the current temperature and T_0 the initial temperature); $\lambda = 2\nu\mu/(1-2\nu)$ and $\mu = G$ are Lame constants of the bulk material; ν is the Poisson's ratio of rock; G is shear modulus. α and M are the Biot's modulus that have the relation $\alpha = 1-K/K_s$ and $1/M = n/K_w + (1-n)/K_s$, where K_s and K_w are the bulk modulus of solid grains and pore fluid, respectively; and $K = \lambda+2\mu/3$ is the drained bulk modulus of the rock medium; λ' is the thermal modulus with the relation $\lambda' = Ka_c$; and a_c is the coefficient of the volumetric expansion of the

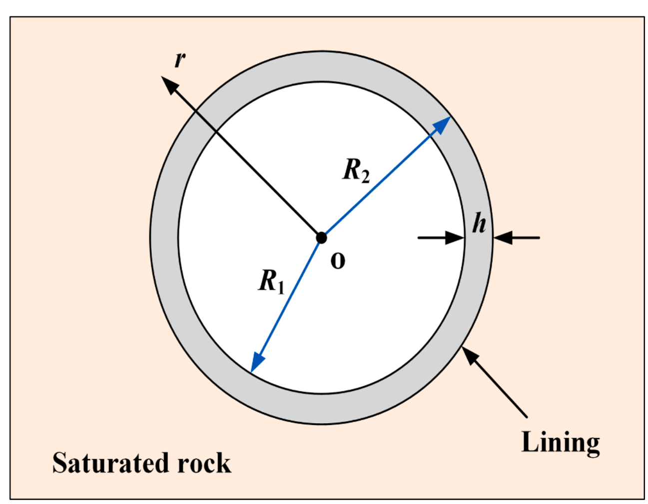

Fig. 1. Model of circular tunnel in saturated rock.

porous medium determined by $a_c = na_w + (1-n)a_s$, n is the porosity of the rock and a_s, a_w are the coefficients of volumetric thermal expansion of the solid grains and the pore fluid, respectively; ∇ is differential operator. ρ_s and ρ_w are the densities of the solid grains and the fluid, respectively; where $\rho = (1-n)\rho_s + n\rho_w$. τ_1 is relaxation time.

With the constitutive relations for linear porothermoelasticity and considering thermal osmosis term in fluid flux (Ghassemi and Diek, 2002), and the inertial effects of solid-fluid interaction (Xia et al., 2017), the equation of fluid flux can be written as (Liu et al., 2009):

$$\kappa\nabla^2 p + D_T\nabla^2\theta = \alpha\frac{\partial e}{\partial t} - a_c\frac{\partial\theta}{\partial t} + \frac{1}{M}\frac{\partial p}{\partial t} + \kappa\rho_w\left(\frac{\alpha}{n} - 1\right)\frac{\partial^2 e}{\partial t^2} - \frac{\kappa\rho_w a_c}{n}\frac{\partial^2\theta}{\partial t^2} + \frac{\kappa\rho_w}{nM}\frac{\partial^2 p}{\partial t^2} \tag{2}$$

where, κ is the mobility coefficient of water, $\kappa = k_l/\rho_w g$, k_l is the intrinsic permeability; g is the gravitational acceleration. The theory of thermoporo-elasticity is also formulated in the terms of 'phenomenological' constants, i.e., D_T, a phenomenological coefficient associated with the influence of thermal gradient on the water flux(thermo-osmosis).

If the property of non-linearity of thermal poroelastic medium is neglected and the change of temperature is small, then the balance equation of heat of the linear, thermal, poroelastic medium can be simplified as following (Liu et al., 2009):

$$m\left(\frac{\partial\theta}{\partial t} + \tau_2\frac{\partial^2\theta}{\partial t^2}\right) - \lambda' T_0\left(\frac{\partial e}{\partial t} + \tau_3\frac{\partial^2 e}{\partial t^2}\right) = S_1\nabla^2\theta + S_2\nabla^2 p + S_3\left[\left(\frac{\alpha}{n} - 1\right)\frac{\partial^2 e}{\partial t^2} + \frac{1}{Mn}\frac{\partial^2 p}{\partial t^2} - \frac{a_c}{n}\frac{\partial^2\theta}{\partial t^2}\right] \tag{3}$$

where, m is the gravimetric specific heat, $m = (1-n)\rho_s C_s + n\rho_w C_w$; C_s and C_w are the specific heats of the solid grains and fluid, respectively. The constants S_1, S_2 and S_3 are $S_1 = k - T_0 a_w K_w D_T$, $S_2 = T_0(D_T - a_w K_w\kappa)$, $S_3 = T_0 a_w K_w \kappa\rho_w$, respectively. k is the thermal conductivity, $k = (1-n)k_s + nk_w$; k_s and k_w are the coefficient of thermal conductivity of solid grains and fluid, respectively. τ_2 and τ_3 are relaxation times.

In order to solve Eqs. (1)–(3), this paper introduces the following dimensionless quantities:

$r^* = V\eta r, u^* = V\eta u, t^* = V^2\eta t, \tau_i^* = V^2\eta\tau_i (i = 1,2,3), \eta = m/k, \theta^* = \lambda'\theta/(\lambda + 2G)$

$$p^* = \alpha p/(\lambda + 2G),\ V = \sqrt{(\lambda + 2G)/\rho} \tag{4}$$

where, V is shear wave velocity.

In terms of these non-dimensional variables, Eqs. (1)–(3) take the following forms, (dropping the asterisks for convenience):

$$\nabla^2 e - \nabla^2 p - \nabla^2\left(\theta + \tau_1\frac{\partial\theta}{\partial t}\right) = \phi_1\frac{\partial^2 e}{\partial^2 t} + \phi_2\frac{\partial^2\theta}{\partial^2 t} + \phi_3\frac{\partial^2 p}{\partial^2 t} \tag{5}$$

$$\nabla^2 p + \varphi_0\nabla^2\theta = \varphi_1\frac{\partial e}{\partial t} + \varphi_2\frac{\partial\theta}{\partial t} + \varphi_3\frac{\partial p}{\partial t} + \varphi_4\frac{\partial^2 e}{\partial t^2} + \varphi_5\frac{\partial^2\theta}{\partial t^2} + \varphi_6\frac{\partial^2 p}{\partial t^2} \tag{6}$$

$$\left(\frac{\partial}{\partial t} + \tau_2\frac{\partial^2}{\partial t^2}\right)\theta + \psi_0\left(\frac{\partial}{\partial t} + \tau_3\frac{\partial^2}{\partial t^2}\right)e = \psi_1\nabla^2\theta + \psi_2\nabla^2 p + \psi_3\frac{\partial^2 e}{\partial t^2} + \psi_4\frac{\partial^2\theta}{\partial t^2} + \psi_5\frac{\partial^2 p}{\partial t^2} \tag{7}$$

where,

$$\phi_1 = \frac{\rho - \rho_w\alpha}{\rho}, \phi_2 = \frac{\rho_w a_c(\lambda + 2G)}{\lambda'\rho}, \phi_3 = -\frac{\rho_w(\lambda + 2G)}{\rho\alpha M} \tag{8}$$

$$\varphi_0 = \frac{D_T\alpha}{\lambda'\kappa},\ \varphi_1 = \frac{\alpha^2}{(\lambda + 2G)\kappa\eta},\ \varphi_2 = -\frac{\alpha a_c}{\lambda'\kappa\eta},\ \varphi_3 = \frac{1}{\kappa\eta M},\ \varphi_4 = \frac{\rho_w\alpha(\alpha - n)}{\rho n} \tag{9}$$

$$\varphi_5 = -\frac{\rho_w a_c\alpha(\lambda + 2G)}{\lambda'\rho n},\ \varphi_6 = \frac{\rho_w(\lambda + 2G)}{\rho M n} \tag{10}$$

$$\psi_0 = -\frac{(\lambda')^2 T_0}{m(\lambda + 2G)},\ \psi_1 = \frac{S_1}{k},\ \psi_2 = \frac{S_2\lambda'}{\alpha k},\ \psi_3 = \frac{S_3\lambda'(\alpha - n)}{\rho k n},\ \psi_4 = -\frac{S_3 a_c(\lambda + 2G)}{n\rho k},\ \psi_5 = \frac{S_3(\lambda + 2G)\lambda'}{\rho k\alpha M n} \tag{11}$$

The technique of Laplace transform is introduced to solve the governing Eqs. (5)–(7), and can be defined as:

$$s^\gamma\overline{f}(s) = \int_0^\infty\frac{\partial^\gamma f(t)}{\partial t^\gamma}e^{-st}\mathrm{d}t \tag{12}$$

Applying Laplace transformation to Eqs. (5)–(7), we can obtain transformed governing equations:

$$(\nabla^2 - s^2\phi_1)\overline{e} = \left[(1 + \tau_1)\nabla^2 + \phi_2 s^2\right]\overline{\theta} + (\nabla^2 + \phi_3 s^2)\overline{p} \tag{13}$$

$$(\nabla^2 - s\varphi_3 - \varphi_6 s^2)\overline{p} = (\varphi_1 s + \varphi_4 s^2)\overline{e} + (\varphi_2 s + \varphi_5 s^2 - \varphi_0\nabla^2)\overline{\theta} \tag{14}$$

$$(s + \tau_2 s^2 - \psi_4 s^2 - \psi_1\nabla^2)\overline{\theta} + \left[\psi_0(s + \tau_3 s^2) - \psi_3 s^2\right]\overline{e} = \left[\psi_2\nabla^2 + \psi_5 s^2\right]\overline{p} \tag{15}$$

where, s is Laplace transform parameter; $\overline{e} = \int_0^\infty e^{-st}e dt$, $\overline{\theta} = \int_0^\infty e^{-st}\theta dt$, $\overline{p} = \int_0^\infty e^{-st}p dt$.

By substituting Eq. (14) and Eq. (15) into Eq. (13), the following expression can be got:

$$\left(\nabla^6 - \xi_1\nabla^4 + \xi_2\nabla^2 - \xi_3\right)(\overline{\theta}, \overline{p}, \overline{e}) = 0 \tag{16}$$

where, ξ_i, $i = 1,2,3$ denotes the s-dependent parameter. Variables ξ_i, $i = 1,2,3$ can be written as:

$$\xi_1 = \frac{\gamma_1\gamma_5 + \psi_1\gamma_6 - \psi_2\gamma_8 + \gamma_3\gamma_7}{\psi_1\gamma_5 + \psi_2\gamma_7} \tag{17}$$

$$\xi_2 = \frac{\gamma_2\gamma_5 + \gamma_1\gamma_6 - \gamma_4\gamma_7 - \gamma_3\gamma_8}{\psi_1\gamma_5 + \psi_2\gamma_7} \tag{18}$$

$$\xi_3 = \frac{\gamma_2\gamma_6 + \gamma_4\gamma_8}{\psi_1\gamma_5 + \psi_2\gamma_7} \tag{19}$$

$$\chi_0 = s + \tau_2 s^2 - \psi_4 s^2 \tag{20}$$

$$\chi_1 = s^2\varphi_6 + s\varphi_3 \tag{21}$$

$$\chi_2 = s\varphi_1 + s^2\varphi_4 \tag{22}$$

$$\chi_3 = s^2\varphi_5 + s\varphi_2 \tag{23}$$

$$\chi_4 = \psi_0(s^2\tau_3 + s) - s^2\psi_3 \tag{24}$$

$$\gamma_1 = \phi_1\psi_1 s^2 + \chi_0 + \chi_4(s\tau_1 + 1) \tag{25}$$

$$\gamma_2 = \chi_0\phi_1 s^2 - \chi_4\phi_2 s^2 \tag{26}$$

$$\gamma_3 = \chi_4 + \psi_2\phi_1 s^2 - \psi_5 s^2 \tag{27}$$

$$\gamma_4 = \chi_4\phi_3 s^2 + \phi_1\psi_5 s^4 \tag{28}$$

$$\gamma_5 = \chi_4 - \chi_2\psi_2 \tag{29}$$

$$\gamma_6 = \chi_4\chi_1 + \chi_2\psi_5 s^2 \tag{30}$$

$$\gamma_7 = \chi_2\psi_1 - \chi_4\psi_0 \tag{31}$$

$$\gamma_8 = \chi_3\chi_4 - \chi_0\chi_2 \tag{32}$$

According to the differential decomposition theory, processing Eq. (16) leads to the following expression:

$$\left(\nabla^2-k_1^2\right)\left(\nabla^2-k_2^2\right)\left(\nabla^2-k_3^2\right)(\bar{\theta},\bar{p},\bar{e})=0 \tag{33}$$

where, k_1, k_2 and k_3 are the characteristic roots of Eq. (16), denoting the velocities of propagation of three possible waves, i.e, the compressional (P_1 and P_2) wave, and thermal (T) wave. Roots k_1, k_2 and k_3 are given by:

$$k_1^2=\frac{1}{3}(2p_1\sin(q_1)+\xi_1) \tag{34}$$

$$k_2^2=\frac{1}{3}\left[\xi_1-p_1\left(\sqrt{3}\cos(q_1)+\sin(q_1)\right)\right] \tag{35}$$

$$k_3^2=\frac{1}{3}\left[\xi_1+p_1\left(\sqrt{3}\cos(q_1)-\sin(q_1)\right)\right] \tag{36}$$

$$p_1=\sqrt{\xi_1^2-3\xi_2} \tag{37}$$

$$q_1=\frac{1}{3}\sin^{-1}\left(-\frac{2\xi_1^3-9\xi_1\xi_2+27\xi_3}{2p_1^3}\right) \tag{38}$$

According to the three kinds of waves P_1, P_2, and T, in saturated porothermoelastic medium, propagation in pore water and soil skeleton, respectively, which were denoted by Liu et al. (2010a). The solution of Eq. (33) can be written as $\bar{\theta}=\bar{\theta}_1+\bar{\theta}_2+\bar{\theta}_3$,$\bar{p}=\bar{p}_1+\bar{p}_2+\bar{p}_3$, and $\bar{e}=\bar{e}_1+\bar{e}_2+\bar{e}_3$. So, Eq. (33) can be decomposed as follows:

$$(\nabla^2-k_1^2)(\bar{\theta},\bar{p},\bar{e})=0\,,(\nabla^2-k_2^2)(\bar{\theta},\bar{p},\bar{e})=0,\ (\nabla^2-k_3^2)(\bar{\theta},\bar{p},\bar{e})=0(\nabla^2-k_3^2)(\bar{\theta},\bar{p},\bar{e})=0 \tag{39}$$

Solving Eq. (39), one obtains:

$$\bar{\theta}=\sum_{i=1}^{3}A_iK_0(k_ir)+\sum_{i=1}^{3}D_iI_0(k_ir) \tag{40}$$

where, $K_0(x)$ is the modified Bessel function of the second kind and order 0, $I_0(x)$ is the modified Bessel function of the first kind and order 0.

Note that $I_0(x)\to\infty$ when $x\to\infty$, so constants D_i should equal to zero. Then, the solutions of Eq. (39), which is bounded at infinity, are given by:

$$\bar{\theta}=\sum_{i=1}^{3}A_iK_0(k_ir) \tag{41}$$

$$\bar{p}=\sum_{i=1}^{3}B_iK_0(k_ir) \tag{42}$$

$$\bar{e}=\sum_{i=1}^{3}C_iK_0(k_ir) \tag{43}$$

where,A_i,B_i, C_i($i=1$, 2, 3) are arbitrary constants.

Since A_i, B_i and C_i are linearly independent constants, the following expression can be acquired by substituting Eqs. (41)–(43) into Eq. (13) and Eq. (14):

$$B_i=\omega_{1i}A_i,\quad C_i=\omega_{2i}A_i \tag{44}$$

where,

$$\omega_{1i}=\frac{(k_i^2+\phi_2s^2)\chi_2+(k_i^2-\phi_1s^2)(\chi_3-\varphi_0k_i^2)}{(k_i^2-\phi_1s^2)(k_i^2-\chi_1)-(k_i^2+\phi_3s^2)\chi_2} \tag{45}$$

$$\omega_{2i}=\frac{(k_i^2-\chi_1)(k_i^2+\phi_2s^2)+(k_i^2+\phi_3s^2)(\chi_3-\varphi_0k_i^2)}{(k_i^2-\phi_1s^2)(k_i^2-\chi_1)-(k_i^2+\phi_3s^2)\chi_2} \tag{46}$$

Integrating both sides of Eq. (43) from zero to infinity, and assuming that $\bar{u}_r$ vanishes at infinity, one obtaines (Liu et al., 2009).

$$\bar{u}_r=-\sum_{i=1}^{3}\frac{C_i}{k_i}K_1(k_ir) \tag{47}$$

Next, by taking the Laplace transform of the established stress-strain constitutive relationship, in which the temperature effect is considered and dimensionless processing, the expressions of stress can be derived:

$$\bar{\sigma}_r=\bar{e}-\beta^2\frac{\bar{u}_r}{r}-\bar{\theta}(1+s\tau_1)-\bar{p} \tag{48}$$

$$\bar{\sigma}_\theta=(1-\beta^2)\bar{e}+\beta^2\frac{\bar{u}_r}{r}-\bar{\theta}(1+s\tau_1)-\bar{p} \tag{49}$$

where, $\beta^2=2G/(\lambda+2G)$, $\bar{\sigma}_r$, $\bar{\sigma}_\theta$ are radial stress and hoop stress of a porous medium, respectively.

By substituting Eqs. (41)–(43) and Eq.(47) into Eq. (48) and Eq. (49), both radial stress and circumferential stress can be expressed as:

$$\bar{\sigma}_r=\sum_{i=1}^{3}\left[\frac{\beta^2}{rk_i}\omega_{2i}K_1(k_ir)+(\omega_{2i}-\omega_{1i}-1-s\tau_1)K_0(k_ir)\right]A_i \tag{50}$$

$$\bar{\sigma}_\theta=\sum_{i=1}^{3}\left\{-\frac{\beta^2}{rk_i}\omega_{2i}K_1(k_ir)+\left[(1-\beta^2)\omega_{2i}-\omega_{1i}-1-s\tau_1\right]K_0(k_ir)\right\}A_i \tag{51}$$

4. Boundary conditions and solutions

The average permeability coefficient of concrete lining is about 1×10^{-8}m/s, and has great effect on the amount of ground water infiltration of tunnel. Due to the relative permeability of lining and rock, the tunnel is partially sealed and the flow boundary condition is partial permeable. The partially permeable property of the tunnel can be denoted approximately with a dimensionless permeability parameter $k_{\rm sl}$ (Li, 1999). Theoretically, the constant $k_{\rm sl}$ ranges between zero and infinite. As $k_{\rm sl}$ approaches to zero, an impermeable lining is recovered and as $k_{\rm sl}$ approaches to a very large value, a permeable lining is obtained.

As the material of lining and rock is assumed to be porous elastic medium, we consider the case of completely flexible lining, the stiffness E_l of lining as it approaches zero. Due to the lining thickness is far smaller than tunnels' radius, i.e., $h<<R_1$, the influence of thickness of the thin lining is neglected. The value of pressure supported by the solid at the boundary of tunnel can be ascertained approximately with the help of stress coefficient τ, i.e. $\tau q(t)$, and that supported by the pore water is $(1-\tau)q(t)$. During the process of carrying out these calculations, whether heat sources and mechanical sources act on the contact surface between the lining and saturated rock ($r=R_2$) or the inner boundary ($r=R_1$) is not distinguished (Liu et al., 2010c). Coupling the property of partial sealing and porosity of tunnel material and geometry, the stress, pore water pressure and temperature increment boundary condition of tunnel can be defined as:

$$\sigma_r=-\tau q(t)\qquad r=R_2 \tag{52}$$

$$\frac{\partial p}{\partial r}=\frac{k_{\rm sl}}{R_2}[p-(1-\tau)q(t)]\qquad r=R_2 \tag{53}$$

$$\theta=T(t)\qquad r=R_2 \tag{54}$$

where, the dimensionless stress coefficient τ (the range of τ is from 0 to 1) that depends on the porosity n of rock was proposed by Liu et al. (2010c) to estimate the water pressure supported by the solid and the pore water pressure, respectively. The coefficient τ is defined as $1-\eta_c$, and η_c, calculated approximately as $\eta_c=n^{2/3}$, is the area coefficient of pore water on the surface of the tunnel due to the poroelastic property of lining and rock. For the concrete material, $\eta_c=2/3$ 1; and the fracture rock $\eta_c\approx1$ (Liu and Xie, 2005). From Eq. (53) and Eq. (54), two extreme boundaries can be obtained, i.e. the inner water pressure is completely supported by the pore water when $\tau \to 0$ and is completely supported by the solid of rock when $\tau \to 1$. There exist also two extreme cases for the parameter k_{sl}, i.e $k_{sl} = k_t/[k_l(\ln R_2 - \ln R_1)]$, in which k_t is the intrinsic permeability of lining (Li, 1999). When $k_{sl} \to 0$, an impermeable lining is recovered and when $k_{sl} \to \infty$, a permeable case is obtained.

The inner water pressure applied on the surface of tunnel, considered herein is assumed to be an axially symmetric with a heat source $q(t)$ and mechanical source $T(t)$. Therefore, $q(t)$ and $T(t)$ can be written as:

$$q(t) = \begin{cases} \sin\left(\dfrac{\pi t}{a_0}\right) & 0 \leqslant t \leqslant a_0 \\ 0 & \text{otherwise} \end{cases} \tag{55}$$

$$T(t) = \begin{cases} \sin\left(\dfrac{\pi t}{a_0}\right) & 0 \leqslant t \leqslant a_0 \\ 0 & \text{otherwise} \end{cases} \tag{56}$$

where, a_0 denotes the amplitude (here, $a_0 = 1$).

By conducting the Laplace transform on Eq. (55) and Eq. (56), the expressions of heat source $q(t)$ and mechanical source $T(t)$ can be derived:

$$\overline{q}(s) = \frac{\pi a_0 (s + e^{-a_0 s})}{a_0^2 s^2 + \pi^2} \tag{57}$$

$$\overline{T}(s) = \frac{\pi a_0 (s + e^{-a_0 s})}{a_0^2 s^2 + \pi^2} \tag{58}$$

By substituting Eqs. (41), (42) and (50) into Eqs. (52)–(54), the following expression can be derived:

$$\sum_{i=1}^{3} \left[\frac{\beta^2}{R_2 k_i} \omega_{2i} K_1(k_i R_2) + (\omega_{2i} - \omega_{1i} - 1 - s\tau_1) K_0(k_i R_2) \right] A_i = -\tau \overline{q}(s) \tag{59}$$

$$\sum_{i=1}^{3} \left[k_i K_1(k_i R_2) + \frac{k_{sl}}{R_2} K_0(k_i R_2) \right] \omega_{1i} A_i = \frac{k_{sl}}{R_2} (1 - \tau) \overline{q}(s) \tag{60}$$

$$\sum_{i=1}^{3} K_0(k_i R_2) A_i = \overline{T}(s) \tag{61}$$

By combining Eqs. (59)–(61), the undetermined coefficients A_1, A_2 and A_3 can be derived, and the thermo-hydro-mechanical coupling dynamic response of the lining tunnel in saturated rock under inner water pressure can be obtained.

5. Degenerate solution of the problem

5.1. Distribution of internal water pressure $q(t)$

When stress coefficient $\tau = 0$, the inner water pressure is completely supported by the pore water pressure. Then, the boundary conditions can be written as:

$$\sigma_r = 0 \qquad r = R_2 \tag{62}$$

$$\frac{\partial p}{\partial r} = \frac{k_{sl}}{R_2} [p - q(t)] \qquad r = R_2 \tag{63}$$

$$\theta = T(t) \qquad r = R_2 \tag{64}$$

Therefore, by substituting Eqs. (41), (42) and (50) into Eqs. (62)–(64), the following expressions can be derived:

$$\sum_{i=1}^{3} \left[\frac{\beta^2}{R_2 k_i} \omega_{2i} K_1(k_i R_2) + (\omega_{2i} - \omega_{1i} - 1 - s\tau_1) K_0(k_i R_2) \right] A_i = 0 \tag{65}$$

$$\sum_{i=1}^{3} \left[k_i K_1(k_i R_2) + \frac{k_{sl}}{R_2} K_0(k_i R_2) \right] \omega_{1i} A_i = \frac{k_{sl}}{R_2} \overline{q}(s) \tag{66}$$

$$\sum_{i=1}^{3} K_0(k_i R_2) A_i = \overline{T}(s) \tag{67}$$

By combining Eqs. (65)–(67), expressions for the undetermined coefficients A_1, A_2 and A_3 can be derived.

When stress coefficient $\tau = 1$, the inner water pressure is completely supported by the solid of rock. Therefore, the stress, pore water pressure and temperature increment boundary condition of the lining tunnel can thus be defined as:

$$\sigma_r = -q(t) \qquad r = R_2 \tag{68}$$

$$\frac{\partial p}{\partial r} = \frac{k_{sl}}{R_2} p \qquad r = R_2 \tag{69}$$

$$\theta = T(t) \qquad r = R_2 \tag{70}$$

Therefore, by substituting Eqs. (39), (40) and (48) into Eqs. (68)–(70), the following expressions can be derived:

$$\sum_{i=1}^{3} \left[\frac{\beta^2}{R_2 k_i} \omega_{2i} K_1(k_i R_2) + (\omega_{2i} - \omega_{1i} - 1 - s\tau_1) K_0(k_i R_2) \right] A_i = -\overline{q}(s) \tag{71}$$

$$\sum_{i=1}^{3} \left[k_i K_1(k_i R_2) + \frac{k_{sl}}{R_2} K_0(k_i R_2) \right] \omega_{1i} A_i = 0 \tag{72}$$

$$\sum_{i=1}^{3} K_0(k_i R_2) A_i = \overline{T}(s) \tag{73}$$

By combining Eqs. (71)–(73), the expressions of undetermined coefficients A_1, A_2 and A_3 can be derived.

5.2. Permeable and impermeable boundary of tunnel

When $k_{sl} \to 0$, the tunnel boundary is completely impermeable, and the boundary conditions can be expressed as:

$$\sigma_r = -\tau q(t) \qquad r = R_2 \tag{74}$$

$$\frac{\partial p}{\partial r} = 0 \qquad r = R_2 \tag{75}$$

$$\theta = T(t) \qquad r = R_2 \tag{76}$$

Therefore, by substituting Eqs. (39), (40) and (48) into Eqs. (74)–(76), the following expressions can be derived:

$$\sum_{i=1}^{3} \left[\frac{\beta^2}{R_2 k_i} \omega_{2i} K_1(k_i R_2) + (\omega_{2i} - \omega_{1i} - 1 - s\tau_1) K_0(k_i R_2) \right] A_i = -\tau \overline{q}(s) \tag{77}$$

$$\sum_{i=1}^{3} [k_i K_1(k_i R_2)] \omega_{1i} A_i = 0 \tag{78}$$

$$\sum_{i=1}^{3} K_0(k_i R_2) A_i = \overline{T}(s) \tag{79}$$

By combining Eqs. (77)–(79), the expressions of undetermined coefficients A_1, A_2 and A_3 can be derived.

When $k_{sl} \to \infty$, the tunnel boundary is completely permeable, and the boundary conditions can be expressed as:

$$\sigma_r = -\tau q(t) \qquad r = R_2 \tag{80}$$

$$p = 0 \qquad r = R_2 \tag{81}$$

$$\theta=T(t)\qquad r=R_2 \tag{82}$$

Therefore, by substituting Eqs. (41), (42) and (50) into Eqs. (80)–(82), the following expressions can be derived:

$$\sum_{i=1}^{3}\left[\frac{\beta^2}{R_2k_i}\omega_{2i}K_1(k_iR_2)+(\omega_{2i}-\omega_{1i}-1-s\tau_1)K_0(k_iR_2)\right]A_i=-\tau\overline{q}(s) \tag{83}$$

$$\sum_{i=1}^{3}K_0(k_iR_2)\omega_{1i}A_i=0 \tag{84}$$

$$\sum_{i=1}^{3}K_0(k_iR_2)A_i=\overline{T}(s) \tag{85}$$

By combining Eqs. (83)–(85), the expressions of undetermined coefficients A_1, A_2 and A_3 can be derived.

6. Numerical results and discussions

In order to derive the expressions for the temperature increment, radial displacement, stress and pore water pressure in the time domain, the effects of both the stress coefficient (τ) and the relative permeability coefficient (k_{sl}) of saturated rock on the dynamic response of the saturated rock were investigated in detail. It is so difficult to obtain the analytical solutions that this study employed the Crump inversion method for finding those numerical solutions.

Assuming the function $F(s)$ denotes the Laplace transform of the function $F(t)$, the Crump inversion in inverse Laplace transform can be expressed as (Crump, 1976):

$$F(t)\approx\frac{e^{at}}{T^*}\left\{\frac{1}{2}F(a)+\sum_{k=1}^{\infty}\left[Re\left[F\left(a+\frac{k\pi i}{T^*}\right)\right]\cos\frac{k\pi t}{T^*}-Im\left[F\left(a+\frac{k\pi i}{T^*}\right)\right]\sin\frac{k\pi t}{T^*}\right]\right\} \tag{86}$$

where $T^*>t/2$. If$|F(t)|\langle Me^{at}$, the error $|\varsigma|\leqslant Me^{v}e^{-2T^*(a-v)}$ (in which $T^*>t/2$).

By referring to Refs. (Liu et al., 2010c) and (Liu et al., 2009), the related parameters in the calculation can be set as below:

$$\begin{aligned}&v=0.35,\ G=1\times10^6\text{Pa},\ \rho_s=2610\text{kg}/\text{m}^3,\ K_w=3.3\text{GPa},k_s\\&=3.29\text{J}/\text{s}\times\text{m}\times^\circ\text{C},\ T_0=300\text{K},\ K_s=59\text{GPa},\ C_w\\&=4186\text{m}^2\cdot\text{s}^{-2}\cdot^\circ\text{C}^{-1},\ a_c=3\times10^{-5\circ}\text{C}^{-1},\ g=9.8\text{m}/\text{s}^2,a_s\\&=3\times10^{-5\circ}\text{C}^{-1},a_w=3\times10^{-4\circ}\text{C}^{-1},\ n=0.4,\ k_l=1\times10^{-8}\text{m}/\text{s},\ k_w\\&=0.582\text{J}/\text{s}\cdot\text{m}\cdot^\circ\text{C},\ C_s=937\text{m}^2/\text{s}^{-2}\cdot^\circ\text{C}^{-1},\ \rho_w=1000\text{kg}/\text{m}^3,\ K\\&=2.95\text{GPa},\ \tau_1=0.05\text{s},\ \tau_2=0.02\text{s},\ \tau_3=0.01\text{s},\ k_{sl}=100,\ \tau=0.4\text{ and }t\\&=1\end{aligned} \tag{87}$$

6.1. Comparative analysis

6.1.1. Case1: Influences of the stiffness of lining

This paper compares the calculation results of the stiff lining with that of the completely flexible lining to analyze the effect of the stiffness of lining. Fig. 2. shows the time history of radial displacement and pore water pressure at the tunnel surface with impermeable boundary condition under the joint action of a sudden constant heat source and mechanical source. Due to the lining is a thin porous material, the displacement of the stiff lining is slightly smaller than that of solution without considering the stiffness of lining. Since this section assumes the tunnel boundary is impermeable, the stiffness of lining less influences the pore water pressure. Therefore, the calculation results of the completely flexible lining are basically reasonable.

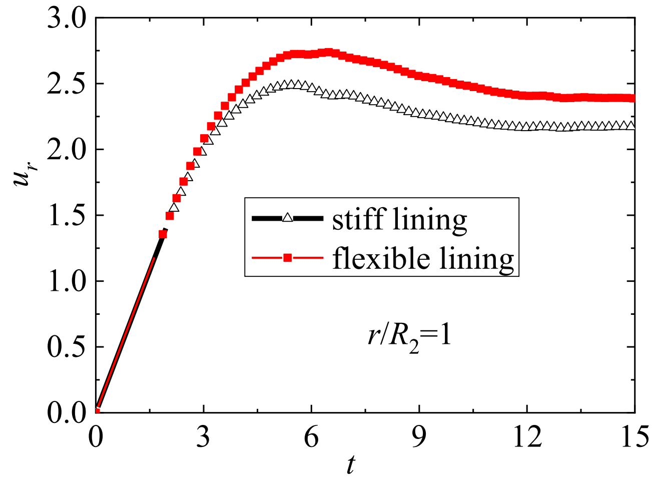

Fig. 2a. The time history of radial displacement for the stiff lining and without stiffness lining cases under the joint action of a sudden constant heat source and mechanical source.

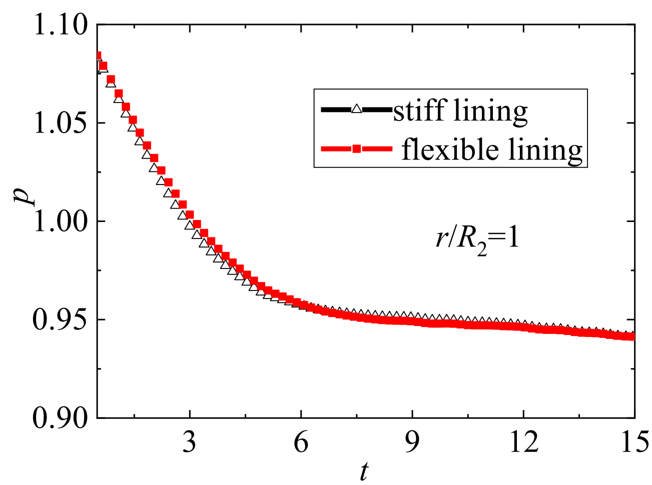

Fig. 2b. The time history of pore water pressure for the stiff lining and without stiffness lining cases under the joint action of a sudden constant heat source and mechanical source.

6.1.2. Case2: Thermo-elastodynamic response

For an ideal thermoelastic medium, there is no fluid in the rock for $\rho_w=0$ and$n=0$, and the governing equations of the coupled thermo-hydro-mechanical response case described in section 3 can also be reduced to that of a general thermoelastic medium (Lord and Shulman, 1967). In addition, when τ_1, τ_2 and τ_3 are zero, and the tunnel boundary is impermeable, the calculation results of this paper can also be reduced to that of Liu's (Liu et al., 2009). Figs. 3 and 4 give the time history of radial displacement of the tunnel with impermeable boundary condition for the results of present work, general thermoelastic theory and Liu's theory, respectively, under a suddenly applied constant mechanical source and heat source. The calculation results for present work, general thermoelastic theory and Liu's theory do not have big differences under a suddenly applied constant mechanical source and heat source. However, for the suddenly applied constant heat source, radial displacement of present work is significantly larger than that of general thermoelastic model because the coefficient of thermal expansion of the fluid is much larger than that of solid. The above comparisons indicate that the derivation in Section 3 is correct, and numerical method is also efficient.

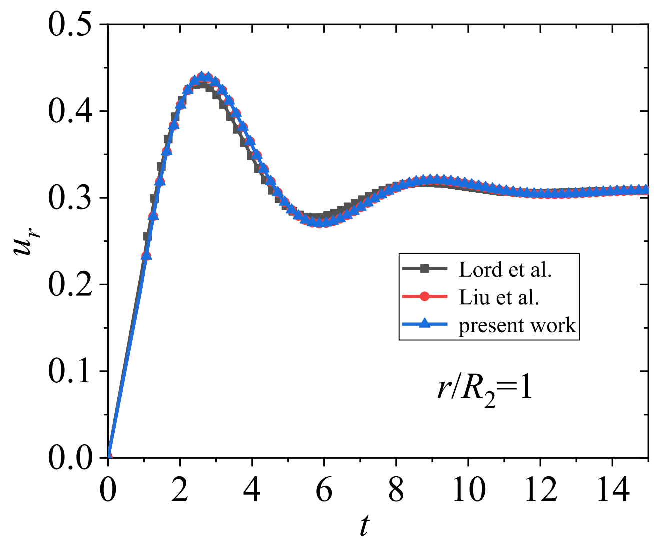

Fig. 3. The time history of radial displacement for present work, Lord's and Liu's cases under a sudden constant mechanical source.

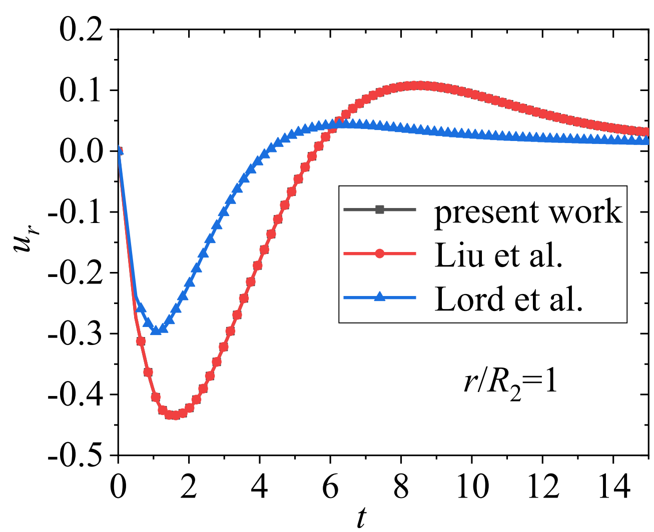

Fig. 4. The time history of radial displacement for present work, Lord's and Liu's cases under a sudden constant heat source.

6.2. Effect of the stress coefficient τ

Fig. 5 displays the variation curves of pore water pressure with the dimensionless radius r/R_2 when the stress coefficient was set to different values ($\tau = 0$, $\tau = 0.4$, $\tau = 0.7$ and $\tau = 1$). Apparently, pore water pressure dropped with the increase of τ. In particular, τ significantly affected pore water pressure at the tunnel boundary (i.e., $r = R_2$). When $\tau = 0$, pore water pressure reaches its maximum because the inner water pressure is completely supported by the pore water pressure. When $\tau = 1$, pore water pressure at the tunnel boundary is almost closing to the zero because the inner water pressure is completely supported by the solid of rock. It is shows that with the increase of τ, the pore pressure gradually increases because the inner water pressure is supported by the pore water pressure gradually reduces.

Fig. 6 shows the variations of radial displacement with the dimensionless radius (r/R_2), when the stress coefficient was set to different values ($\tau = 0$,$\tau = 0.4$, $\tau = 0.7$ and $\tau = 1$). It can be observed that stress coefficient τ most significantly affect radial displacement. Furthermore, with the increase of τ, the radial displacement at the tunnel boundary gradually increased because the inner water pressure is supported by the solid of rock gradually increases. However, at approximately $r/R_2 = 1.6$, the effect of τ on radial displacement changed abruptly. When $1.6 \leqslant r/R_2 \leqslant 2.5$, radial displacement dropped gradually with the increase of τ. At approximately$r/R_2 > 2.5$, τ had almost no effect on radial displacement. The phenomenon may be due to the interaction between thermo-hydro-mechanical in the saturated rock.

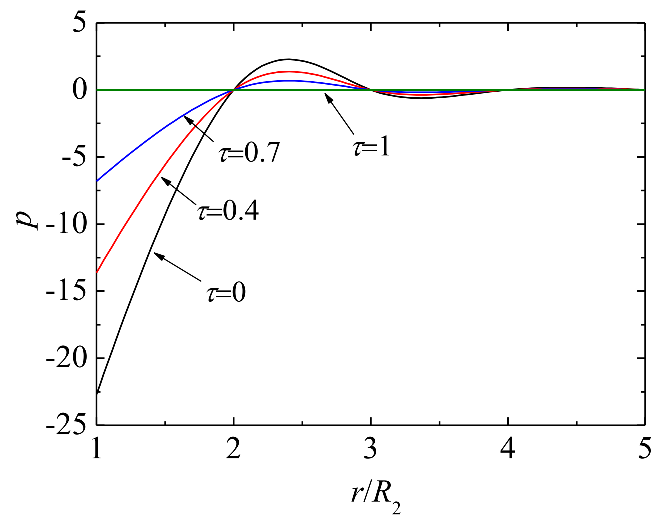

Fig. 5. Variations of pore water pressure with the dimensionless radius when $\tau = 0$, $\tau = 0.4$, $\tau = 0.7$ and $\tau = 1$.

Fig. 7 shows the laws of circumferential stress variation with respect to the dimensionless radius (r/R_2), when the stress coefficient was set to different values ($\tau = 0$,$\tau = 0.4$, $\tau = 0.7$ and $\tau = 1$). The value of τ had significant effects on the circumferential stress at the interface between soil and lining (i.e., $r = R_2$). As the dimensionless radius r/R_2 increased, τ imposed decreasing effects on circumferential stresses, and simultaneously, circumferential stress dropped steadily.

Fig. 8 shows the laws of temperature increment variation with respect to the dimensionless radius (r/R_2) when the stress coefficient was set to different values ($\tau = 0$, $\tau = 0.4$, $\tau = 0.7$ and $\tau = 1$). Apparently, the stress coefficient τ had almost no effect on temperature increment whether inner water pressure is supported by pore water pressure or is supported by the solid of rock.

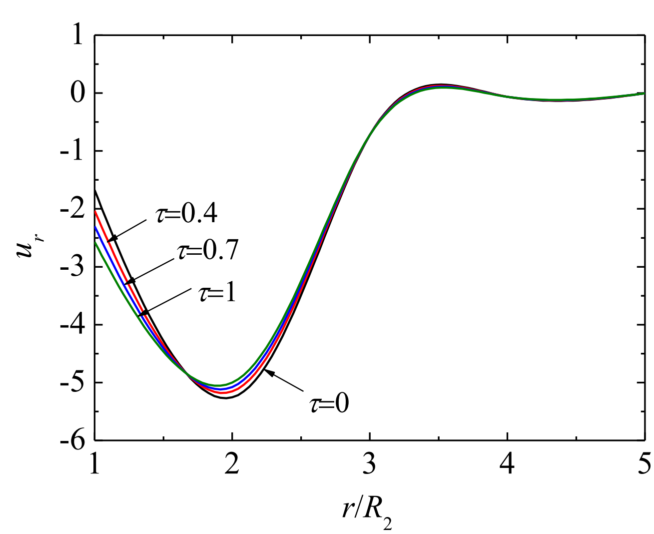

Fig. 6. Variations of radial displacement with the dimensionless radius when $\tau = 0$, $\tau = 0.4$, $\tau = 0.7$ and $\tau = 1$.

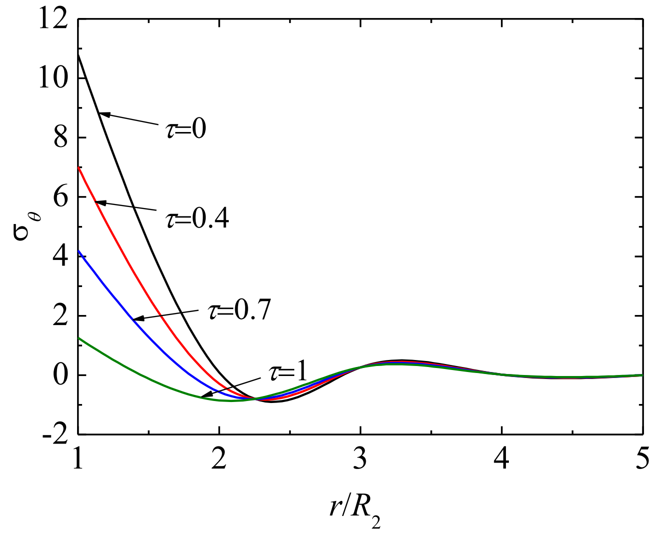

Fig. 7. Variations of circumferential pressure with the dimensionless radius when $\tau = 0$, $\tau = 0.4$, $\tau = 0.7$ and $\tau = 1$.

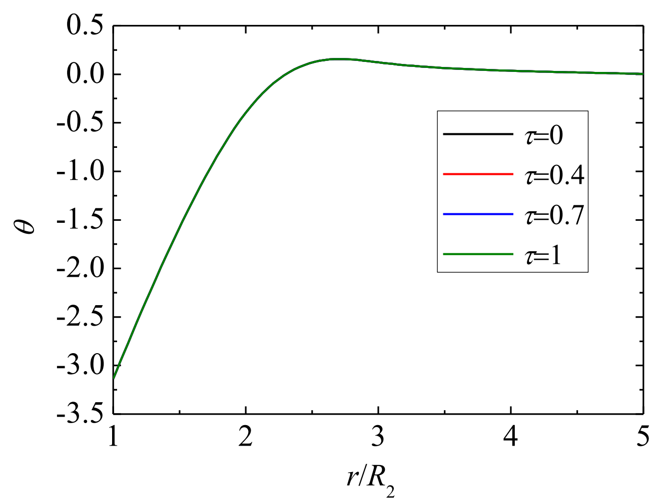

Fig. 8. Variations of temperature increment with the dimensionless radius when $\tau = 0$, $\tau = 0.4$, $\tau = 0.7$ and $\tau = 1$.

6.3. *Effect of relative permeability coefficient k_{sl}*

Fig. 9 displays the rules of variations of the radial displacement with the dimensionless radius at the moment $t = 1$ when the relative permeability coefficient is set to different values ($k_{sl} = 0.01$, $k_{sl} = 1$, $k_{sl} = 100$ and $k_{sl} = 10000$), during which the other parameters are set according to Eq. (86). It can be easily observed that relative permeability coefficient significantly affected radial displacement under hot water pressure. At the interface between lining and soil (i.e., $r = R_2$), radial displacement increases gradually with the increase of the relative permeability coefficient, which suggests that displacement related to the permeability at the boundary. However, the displacements at $k_{sl} = 0.01$ and $k_{sl} = 1$ are close to each other. This is due to the fact that the interface between linings and soils begin to be impermeable. When $k_{sl} = 10000$, the displacement is positive at the interface between lining and soil (i.e., the structure was stretched), and the displacement become negative at $2 < r/R_2 < 3$ (i.e., the structure is compressed). It suggests that radial displacement fluctuate when the boundary approached permeable. Furthermore, permeability and impermeability are the only two limiting conditions at the tunnel boundary.

Fig. 10 displays the rules of variations of the pore water pressure

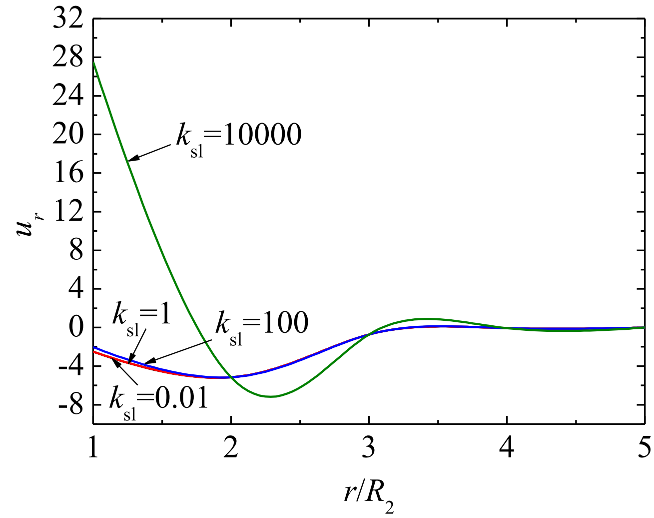

Fig. 9. Variations of radial displacement with the dimensionless radius when $k_{sl} = 0.01$, $k_{sl} = 1$, $k_{sl} = 100$ and $k_{sl} = 10000$.

with the dimensionless radius as the moment $t = 1$ when the relative permeability coefficient is set to different values ($k_{sl} = 0.01$,$k_{sl} = 1$, $k_{sl} = 100$ and $k_{sl} = 10000$, respectively), during which the other parameters are set according to Eq. (87). Under hot water pressure, the boundary permeability has a great deal of effect on the pore water pressure. At the interface between lining and soil (i.e., $r = R_2$), the pore water pressure increases gradually with the increasing of relative permeability coefficient. However, at $k_{sl} = 0.01$ and$k_{sl} = 1$, pore water pressure imposes slight effects. This is because that the boundary is already closed, i.e., the boundary is impermeable.

Fig. 11 displays the rules of variations of the temperature increment with the dimensionless radius at the moment $t = 1$ when the relative permeability coefficient is set to different values ($k_{sl} = 0.01$,$k_{sl} = 1$, $k_{sl} = 100$ and $k_{sl} = 10000$, respectively), during which the other parameters are set according to Eq. (87). It can be easily observed that the temperature increment is irrelevant to the relative permeability coefficient of the lining-soil boundary. With the increase of the relative permeability coefficient, the temperature increments remain almost unchanged.

Fig. 12 displays the rules of variations of the circumferential stress with the dimensionless radius at the moment $t = 1$ when the relative permeability coefficient is set to different values ($k_{sl} = 0.01$, $k_{sl} = 1$,

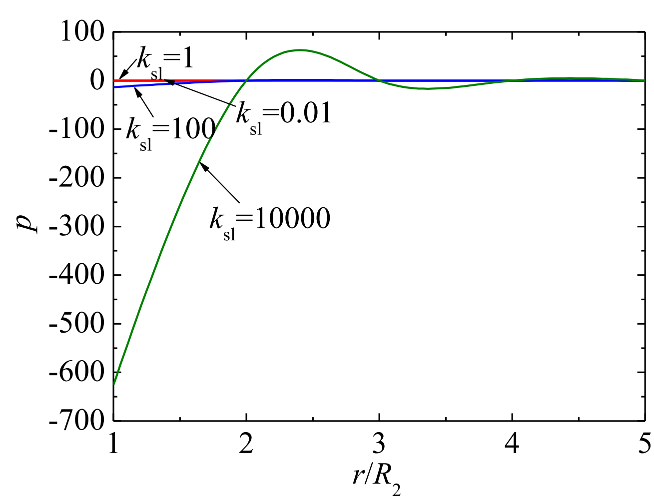

Fig. 10. Variations of pore water pressure with the dimensionless radius when $k_{sl} = 0.01$, $k_{sl} = 1$, $k_{sl} = 100$ and $k_{sl} = 10000$.

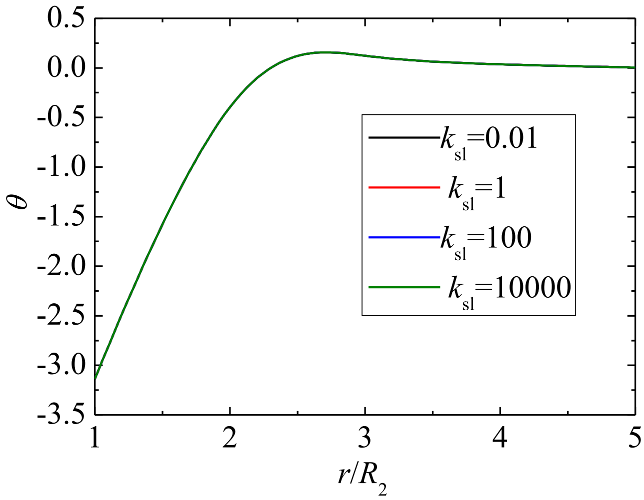

Fig. 11. Variations of temperature increment with the dimensionless radius when $k_{sl} = 0.01$, $k_{sl} = 1$, $k_{sl} = 100$ and $k_{sl} = 10000$.

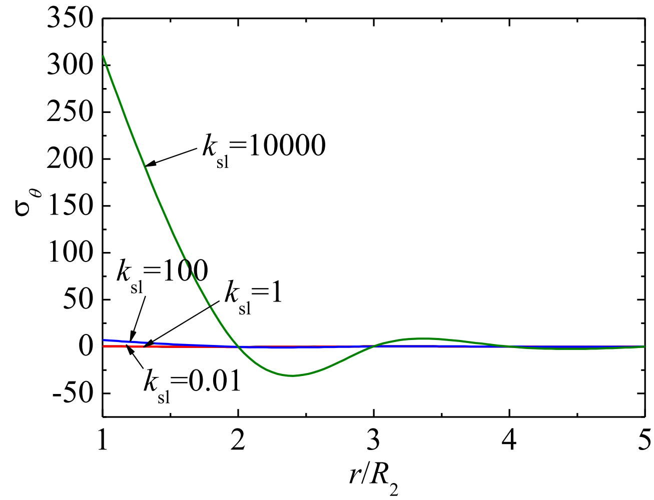

Fig. 12. Variations of circumferential stress with the dimensionless radius when $k_{sl} = 0.01$, $k_{sl} = 1$, $k_{sl} = 100$ and $k_{sl} = 10000$.

$k_{sl} = 100$ and $k_{sl} = 10000$, respectively), during which the other parameters are set according to Eq. (87). The circumferential stress increases gradually with the increase of the relative permeability coefficient at the interface between lining and soil ($r = R_2$). However, the circumferential stresses at $k_{sl} = 0.01$ and $k_{sl} = 1$ exhibites slight differences. This can be attributed to the fact that the boundary began to close, i.e., the boundary is impermeable.

7. Conclusions

The thermo-hydro-mechanical response of a partially sealed circular tunnel in an isotropic, saturated porous rock is analyzed when the surface of the tunnel is subjected to a time dependent heat and mechanical source. A partially sealed boundary condition is used to model water flow across the tunnel-rock interface. A stress coefficient depending on the volume fraction of the pore fluid is quoted to establish the stress coordination conditions at the boundary of tunnel, and the solutions of temperature increment, displacement, pore water pressure and stress are obtained in the domain of Laplace transform. The influences of permeable coefficient and stress coefficient on the response are discussed. The results provide a rational method for the design of high temperature tunnel since some important parameters are considered. However, the model is one dimensional because of the axisymmetric loading and the governing equations of the thermo-hydro-mechanical response are restricted to those cases that within the scope of the analysis e.g. linear elasticity.

By introducing a stress coefficient to model the interface between lining and rock, the modeling problem of inner water pressure supported by the boundary of tunnel can be effectively addressed, and the viewpoint that inner water pressure is sheared by lining and rock is proposed.

A dimensionless permeable parameter defines the flow capacity of the lining, is introduced by considering the relative permeability of the lining of the tunnel and the surrounding rock. The available result without considering the properties of partial sealing and porosity is only an extreme case of this paper.

Declaration of Competing Interest

The authors declare that they have no known competing financial interests or personal relationships that could have appeared to influence the work reported in this paper.

Acknowledgments

Financial support for this study was provided by the National Natural Science Foundation of China (Grand Nos. 52108347, 52179112, 52178371), the Exploring Youth Project of Zhejiang Natural Science Foundation (Grant No. LQ22E080010), the Construction Research Founds of Department of Housing and Urban-Rural Development of Zhejiang Province (Grant No. 2021K256). These support are gratefully acknowledged.

Appendix A. Supplementary data

Supplementary data to this article can be found online at https://doi.org/10.1016/j.tust.2022.104552.

References

Abouelregal, A.E., 2013. Generalized thermoelastic infinite transversely isotropic body with a cylindrical cavity due to moving heat source and harmonically varying heat. Meccanica 48 (7), 1731–1745.

Abousleiman, Y., Ekbote, S., 2005. Solutions for the inclined borehole in a porothermoelastic transversely isotropic medium. J. Appl. Mech-T. Asme 72, 102–114.

Bai, B., Li, T., 2013. Irreversible consolidation problem of a saturated porothermoelastic spherical body with a spherical cavity. Appl. Math. Modell. 37 (4), 1973–1982.

Bai, M., Abousleiman, Y., 1997. Thermoporoelastic coupling with application to consolidation. Int. J. Numer. Anal. Methods Geomech. 21 (2), 121–132.

Biot, M.A., 1977. Variational Lagrangian-thermodynamics of nonisothermal finite strain mechanics of porous solids and thermomolecular diffusion. Int. J. Soilds Struct. 13 (6), 579–597.

Blond, E., Schmitt, N., Hild, F., 2003. Response of saturated porous media to cyclic thermal loading. Int. J. Numer. Anal. Methods Geomech. 27 (11), 883–904.

Crump, K.S., 1976. Numerical inversion of Laplace transforms using a Fourier series approximation. J. ACM 23 (1), 89–96.

Ezzat, M., Ezzat, S., 2016. Fractional thermoelasticity applications for porous asphaltic materials. Pet. Sci. 13 (3), 550–560.

Ezzat, M.A., 2011. Theory of fractional order in generalized thermoelectric MHD. Appl. Math. Modell. 35 (10), 4965–4978.

Gao, M., Wang, Y., Gao, G.Y., Yang, J., 2013. An analytical solution for the transient response of a cylindrical lined cavity in a poroelastic medium. Soil Dyn. Earthquake Eng. 46, 30–40.

Gao, M., Zhang, J.Y., Chen, Q.S., Gao, G.Y., Yang, J., Li, D.Y., 2016. An exact solution for three-dimensional (3D) dynamic response of a cylindrical lined tunnel in saturated soil to an internal blast load. Soil Dyn. Earthquake Eng. 90, 32–37.

Green, A.E., Lindsay, K.A., 1972. Thermoelasticity. J. Elast. 2 (1), 1–7.

Green, A.E., Naghdi, P.M., 1993. Thermoelasticity without energy dissipation. J. Elast. 31 (3), 189–208.

Ghassemi, A., Diek, A., 2002. Porothermoelasticity for swelling shales. J Petro Sci Eng 34 (1), 123–135.

Hamza, F., Abdou, M., Abd El-Latief, A.M., 2014. Generalized Fractional Thermoelasticity Associated with Two Relaxation Times. J. Therm. Stresses 37 (9), 1080–1098.

Hamza, F., Abd El-Latief, A.M., Abdou, M., 2016. 1D applications on fractional generalized thermoelasticity associated with two relaxation times. Mech. Adv. Mater. Struct. 23 (6), 689–703.

He, L.W., Yang, X., 2009. Quasi-static and dynamic behavior of incompressible saturated poroelastic one-dimensional column on local thermal non-equilibrium. J. Mech. MEMS. 1, 289–299.

Kundu, M.R., Mukhopadhyay, B., 2005. A thermoviscoelastic problem of an infinite medium with a spherical cavity using generalized theory of thermoelasticity. Math. Comput. Modell. 41 (1), 25–32.

Li, X., 1999. Stress and displacement fields around a deep circular tunnel with partial sealing. Comput. Geotech. 24 (2), 125–140.

Liu, G., Xie, K., Ye, R., 2010a. Mode of a spherical cavity's thermo-elastodynamic response in a saturated porous medium for non-torsional loads. Computers Geotechnics 37 (3), 381–390.

Liu, G., Liu, X., Ye, R., 2010b. The relaxation effects of a saturated porous media using the generalized thermoviscoelasticity theory. Int. J. Eng. Sci. 48 (9), 795–808.

Liu, G.B., Xie, K.H., 2005. Transient response of a spherical cavity with a partially sealed shell embedded in viscoelastic saturated soil. J. Zhejiang Univ. Sci. 6A (3), 194–201.

Liu, G.-B., Xie, K.-h., Liu, X., 2010c. Dynamic response of a partially sealed tunnel in porous rock under inner water pressure. Tunn. Undergr. Space Technol. 25 (4), 407–414.

Liu, G.B., Xie, K.H., Zheng, R.Y., 2009. Model of nonlinear coupled thermo-hydro-elastodynamics response for a saturated poroelastic medium. Sci. China Ser. E: Technol. Sci. 52 (8), 2373–2383.

Lord, H.W., Shulman, Y., 1967. A generalized dynamical theory of thermoelasticity. J. Mech. Phys. Solids. 15 (5), 299–309.

Lu, J.F., Jeng, D.S., Lee, T.L., 2007. Dynamic response of a piecewise circular tunnel embedded in a poroelastic medium. Soil Dyn. Earthquake Eng. 27 (9), 875–891.

Senjuntichai, T., Rajapakse, R.K.N.D., 2010. Transient response of a circular cavity in a poroelastic medium. Int. J. Numer. Anal. Methods Geomech. 17 (6), 357–383.

Sherief, H.H., Hussein, E.M., 2012. A Mathematical Model for Short-Time Filtration in Poroelastic Media with Thermal Relaxation and Two Temperatures. Transp. Porous Media 91 (1), 199–223.

Xia, R.H., Tian, X.G., Shen, Y.P., 2009. The influence of diffusion on generalized thermoelastic problems of infinite body with a cylindrical cavity. Int. J. Eng. Sci. 47 (5–6), 669–679.

Xia, Y., Jin, Y., Chen, M., Chen, K.P., 2017. Poroelastodynamic response of a borehole in a non-hydrostatic stress field. Int. J. Rock Mech. Min. Sci. 93, 82–93.

Xie, K.H., Liu, G.B., Shi, Z.Y., 2004. Dynamic response of partially sealed circular tunnel in viscoelastic saturated soil. Soil Dyn. Earthquake Eng. 24 (12), 1003–1011.

Xiong, C., Guo, Y., Yu, D., 2018. Dynamic Responses of Saturated Porous Foundations Under Coupled Thermo-Hydro-Mechanical Effects. Appl. Math. Mech. 39, 689–699.

Yang, X., 2005. Gurtin-type variational principles for dynamics of a non-local thermal equilibrium saturated porous medium. Acta Mech. Solida Sin. 18, 40–48.

Youssef, H.M., 2011. Theory of Two-Temperature Thermoelasticity without Energy Dissipation. J. Therm. Stresses 34 (2), 138–146.